

Supporting Information

SnO₂ Patched Ultrathin PtRh Nanowires as Efficient Catalysts for Ethanol Electrooxidation

*Xiaokun Fan^a, Min Tang^b, Xiaotong Wu^a, Shuiping Luo^b, Wen Chen^b, Xing Song^b and
Zewei Quan^{b*}*

^aSchool of Chemical Biology and Biotechnology, Shenzhen Graduate School, Peking
University, Shenzhen, Guangdong 518055, China

^bDepartment of Chemistry, Southern University of Science and Technology
(SUSTech), Shenzhen, Guangdong 518055, China

***Correspondence author.** E-mail: quanzw@sustech.edu.cn

Experimental section:

Chemicals.

Platinum(II) acetylacetonate ($\text{Pt}(\text{acac})_2$, 98%) and nickel(II) acetylacetonate ($\text{Ni}(\text{acac})_2$, 98%) were purchased from Energy Chemical. Oleylamine (OAm, 70%) and hexadecyltrimethylammonium bromide (CTAB, $\geq 99.0\%$) were purchased from Sigma-Aldrich. Tin chloride dihydrate ($\text{SnCl}_2 \cdot 2\text{H}_2\text{O}$, 98.0%) and ruthenium(III) acetylacetonate ($\text{Ru}(\text{acac})_3$, 97%) were purchased from Aladdin. Rhodium(III) acetylacetonate ($\text{Rh}(\text{acac})_3$, 97%) was purchased from Macklin. Hexacarbonyl tungsten ($\text{W}(\text{CO})_6$, 97%) was purchased from Alfa Aesar. N-hexane (97%) and ethanol absolute ($\geq 99.7\%$) were purchased from Yonghua Chemical Technology Co., Ltd. (Jiangsu, China). All the chemicals were used as received without further purification. The water (18.2 M Ω /cm) used in all experiments was prepared by passing through an ultra-pure purification system (Master-Q 15UT, HHitech).

Synthesis of SnO_2 patched ultrathin PtRh nanowires ($\text{PtRh}@ \text{SnO}_2$ NWs).

In a typical synthesis of ultrathin $\text{PtRh}@ \text{SnO}_2$ NWs, $\text{SnCl}_2 \cdot 2\text{H}_2\text{O}$ (11.5 mg) was first dissolved into 2 mL of OAm by sonication. $\text{Pt}(\text{acac})_2$ (20.0 mg), $\text{Rh}(\text{acac})_3$ (5.0 mg), CTAB (185.0 mg) and 8 mL of OAm were added into a three-neck flask. The mixture was heated up to 130 °C with vigorous stirring under an argon stream. Subsequently, 50.0 mg of $\text{W}(\text{CO})_6$ was introduced into the homogeneous solution, and the reaction temperature was then raised to 240 °C quickly. When the temperature reached 240 °C, the stock solution of Sn precursors was injected into three-neck flask quickly, and the mixed solution was kept at 240 °C for 3 h. The cooled product was collected by centrifugation and washed twice with an ethanol/n-hexane (volume ratio, 1:4) mixture. The final NWs were re-dispersed in n-hexane. The SnO_2 content can be tuned by changing the amount of Sn precursor. Keeping the other conditions unchanged, $\text{PtRh}@ \text{SnO}_2$ NWs with 26.8 at.% and 48.6 at.% Sn were synthesized by adding 5.8 mg and 17.3 mg of $\text{SnCl}_2 \cdot 2\text{H}_2\text{O}$, respectively.

Synthesis of SnO_2 patched ultrathin Pt NWs ($\text{Pt}@ \text{SnO}_2$ NWs), PtNi NWs ($\text{PtNi}@ \text{SnO}_2$ NWs) and PtRu NWs ($\text{PtRu}@ \text{SnO}_2$ NWs).

The preparations of ultrathin $\text{Pt}@ \text{SnO}_2$, $\text{PtNi}@ \text{SnO}_2$ and $\text{PtRu}@ \text{SnO}_2$ NWs were similar to that of ultrathin $\text{PtRh}@ \text{SnO}_2$ NWs except adding different acetylacetonate compounds [$\text{Ni}(\text{acac})_2$ (13.1 mg) or $\text{Ru}(\text{acac})_3$ (10.0 mg)].

Synthesis of ultrathin Pt NWs.

Ultrathin Pt NWs were prepared by the one-pot synthesis method we reported recently.¹

The annealing treatment of ultrathin NWs.

The as-synthesized ultrathin NWs were first loaded onto commercial carbon (Vulcan XC72 carbon) by sonication for 2 h to avoid the aggregation of NWs during the annealing. Subsequently, the products were collected by centrifugation and washed twice with 10 mL of ethanol. These products were re-dispersed in 10 mL of ethanol and dried in vacuum at 60 °C for 5 h; the resulting pulverized samples were annealed at 200 °C for 1 h in air. This approach could also remove the remaining ligands on the surface of NWs, and the as-prepared products can be used as the catalyst for the final ethanol oxidation reaction (EOR) tests directly.

Characterizations

The transmission electron microscope (TEM) images of different NWs were obtained by Hitachi HT7700 (100 kV) and FEI Talos F200X TEM (200 kV). Aberration-corrected high-angle annular dark-field scanning transmission electron microscopy (HAADF-STEM) were conducted on a FEI Titan Cubed Themis G2 (300 kV) equipped with a spherical aberration corrector for the objective lens. X-ray diffraction (XRD) patterns were recorded by an X-ray diffractometer (Rigaku SmartLab) with Cu K α radiation ($\lambda = 0.15418$ nm). X-ray photoelectron spectroscopy (XPS) was performed on a PHI 5000 Versaprobe III XPS spectrometer with Al K α as the excitation source. The composition of NWs and concentration of catalysts were measured by energy-dispersive X-ray spectroscopy (EDX, FEI Talos F200X) and inductively coupled plasma mass spectrometry (ICP-MS, Agilent 7700x).

Electrochemical Tests

Before the electrochemical tests, 1 mg of the as-prepared catalysts were re-dispersed in 1 mL of mixture solvent containing ultrapure water, isopropanol and Nafion (5%) (volume ratio, 1:1:0.008) to obtain a homogeneous catalyst ink by sonication for 1 h. A typical three-electrode electrochemical cell was used to perform the EOR measurements. A glassy-carbon electrode (diameter: 5 mm) was used as the working electrode, a platinum foil (1 cm * 1 cm) as the counter electrode, and a saturated calomel electrode (SCE) as the reference electrode. Electrochemical measurements were conducted via a biopotentiostat (AFCBP1E, Pine Instrument Co., USA) at room temperature. The Pt loadings of catalysts on the glassy-carbon electrode were controlled to be 0.1 mg_{Pt} mL⁻¹ based on ICP-MS analysis. 10 μ L of the catalyst ink was dropped onto the GC-RDE and dried under ambient condition. As a standard, 10 μ L of the commercial Pt/C (20 wt.% Pt, HISPEC3000, JM) ink was also dispersed on glassy-carbon electrode with a loading amount of 10.2 μ g cm⁻². The electrochemical active surface areas (ECSAs) were estimated by integrating the hydrogen adsorption charge on the cyclic voltammetry (CV) in an Ar-saturated 1 M NaOH solution at a scan rate of 50 mV s⁻¹ between -1.0–0.1 V vs SCE. EOR activities were measured in an Ar-saturated 1 M NaOH + 1 M ethanol at a scan rate of 50 mV s⁻¹ between -1.0–0.1 V vs SCE when the CV cycles were stable (normally 20 cycles). For the EOR stability tests, chronoamperometry experiments were carried out at a constant potential of -0.60 V vs

SCE for 1000 s.

CO-stripping tests were performed in a 1 M NaOH solution. Before the tests, to saturate the surface of catalysts, CO was bubbled into the cell for 15 min while the potential of the working electrode was held at a constant potential of -0.88 V vs SCE, and then Ar was bubbled into the solution for 15 min to remove the remaining CO gas. Afterwards, the CO-stripping curves were recorded by sweeping from -1.0 to 0.1 V vs SCE at a scan rate of 50 mV s⁻¹.

Supplementary Figures

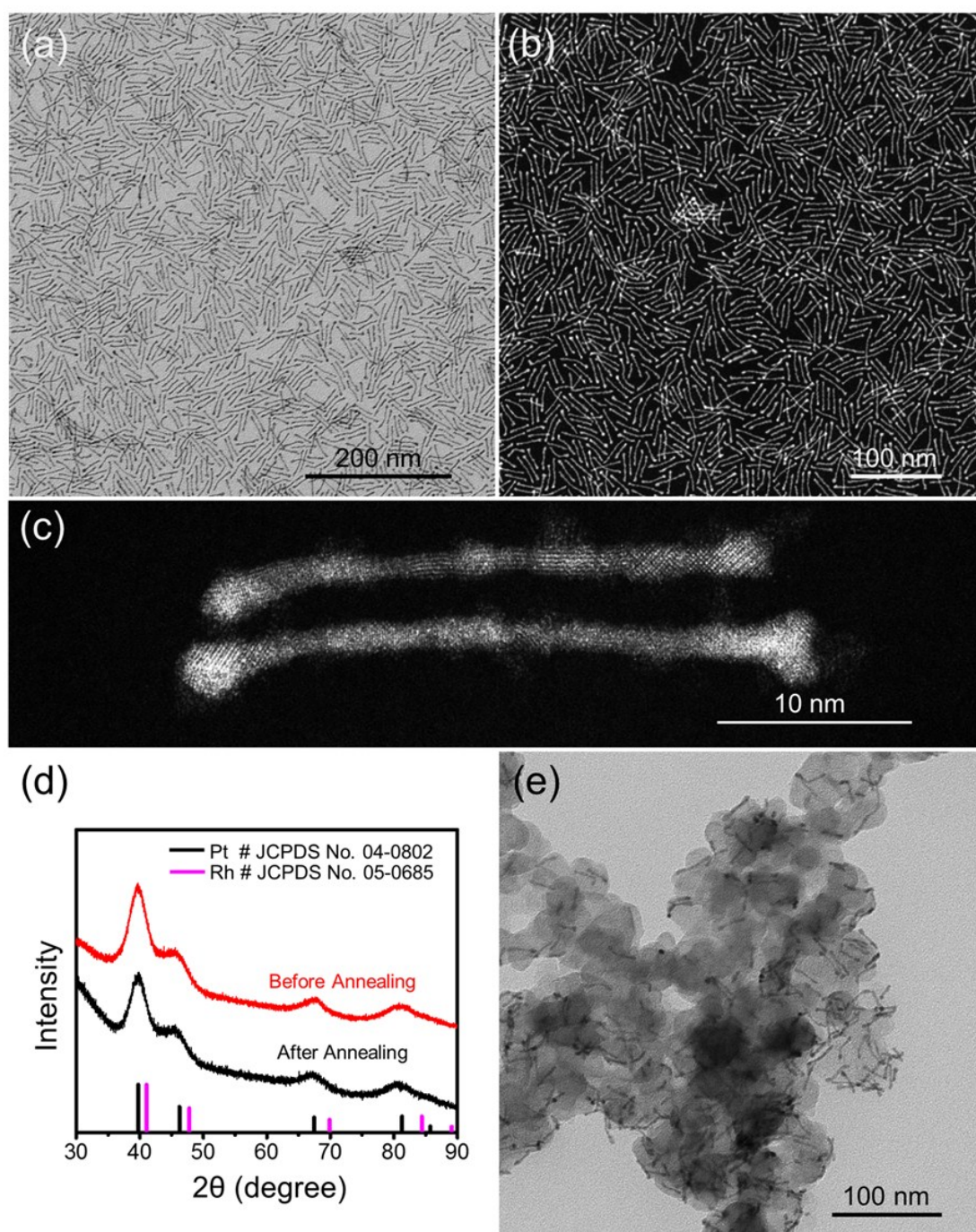


Figure S1. Additional (a) TEM, (b) HAADF-STEM, and (c) aberration-corrected HAADF-STEM images of ultrathin PtRh@SnO₂ NWs. (d) XRD pattern and (e) TEM images of ultrathin PtRh@SnO₂ NWs on commercial carbon after annealing treatment. (c) demonstrates that the darker atoms randomly spread around the surface of inner NWs. (d) and (e) indicate the annealing treatment have little influence on the morphology and crystal structure as-prepared NWs.

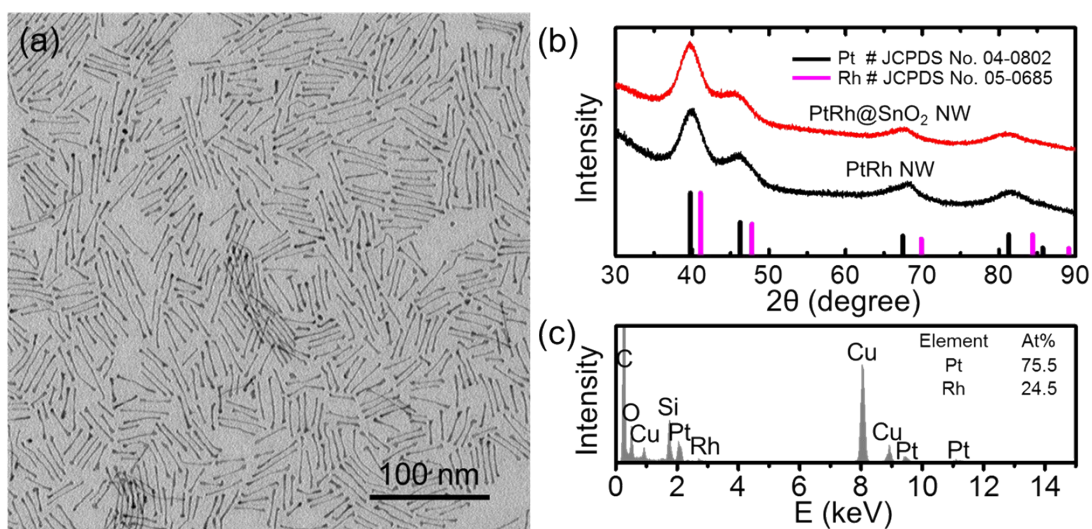


Figure S2. (a) TEM image, (b) XRD pattern and (c) EDX spectrum of PtRh NWs obtained at 240 °C before adding the Sn precursor.

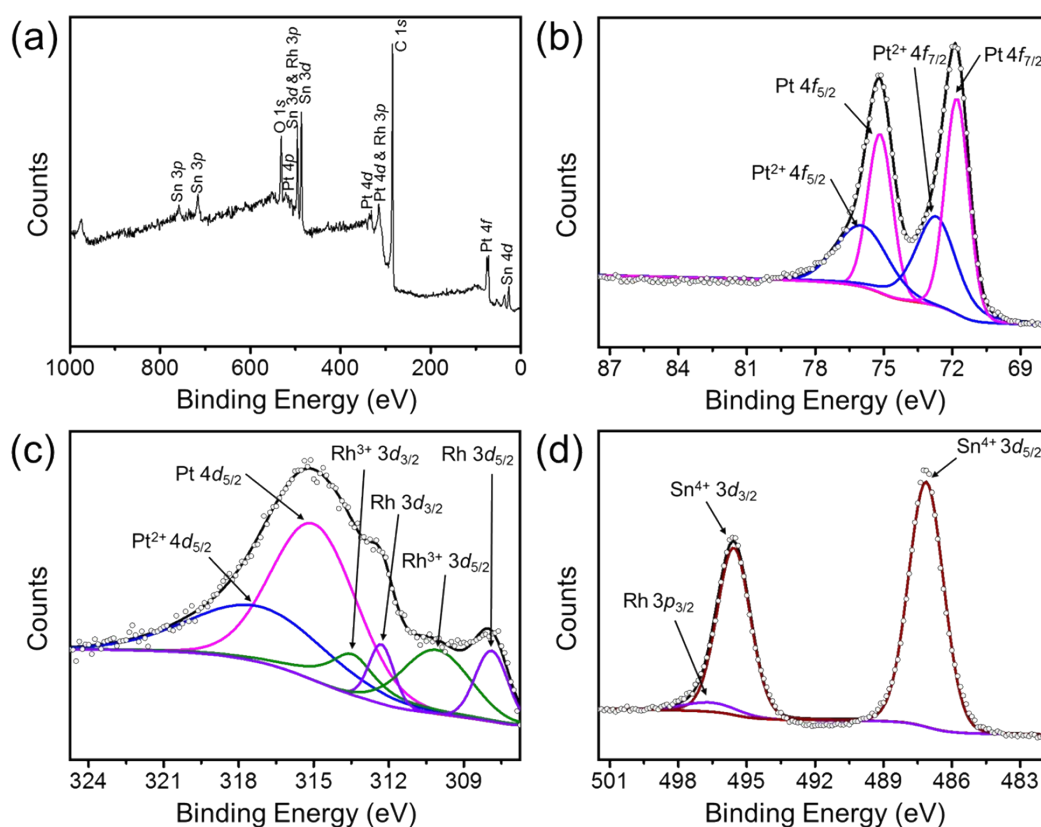


Figure S3. (a) XPS survey spectrum of ultrathin PtRh@SnO₂ NWs on commercial carbon before annealing treatment. Corresponding high-resolution XPS spectra of (b) Pt 4f, (c) Rh 3d, and (d) Sn 3d. These results indicate Sn atoms have been oxidized to Sn⁴⁺ completely before annealing, which is probably for the residual air in the synthesis system.

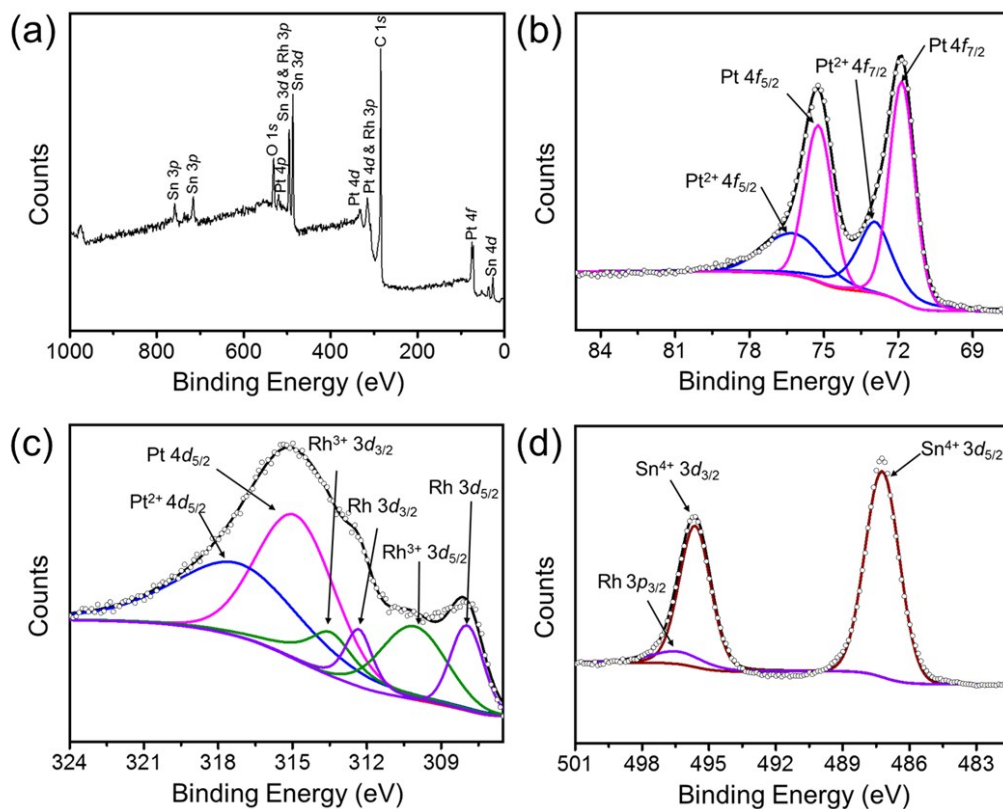


Figure S4. (a) XPS survey spectrum of ultrathin PtRh@SnO₂ NWs on commercial carbon after annealing treatment. Corresponding high-resolution XPS spectra of (b) Pt 4f, (c) Rh 3d, and (d) Sn 3d.

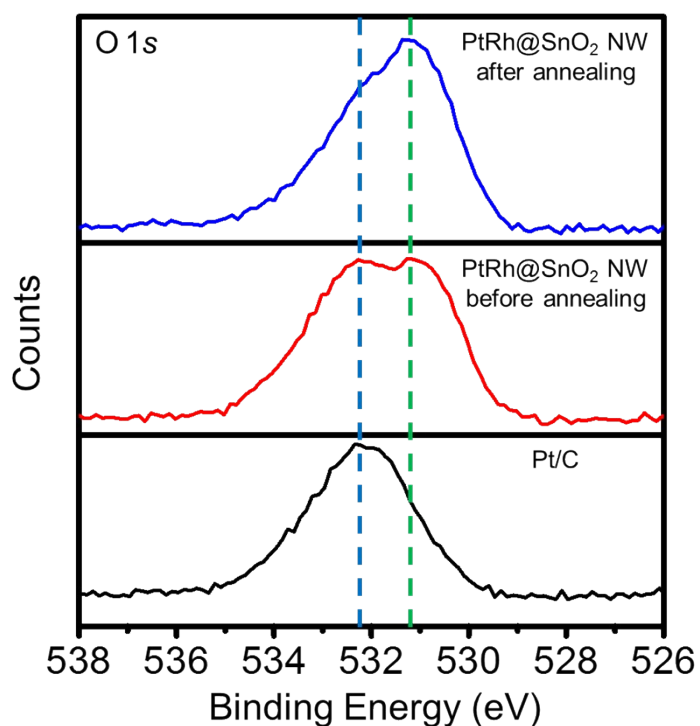


Figure S5. The O 1s XPS spectra of commercial Pt/C and PtRh@SnO₂ NW/C before and after annealing. The O 1s XPS results of PtRh@SnO₂ NWs before and after annealing can be divided into two parts. The first one at ~532.2 eV originates from the absorbed H₂O, O₂ and CO₂ on the carbon and catalyst surface, which is also observed in the O 1s spectrum of commercial Pt/C.^{2, 3} The second one at ~531.1 eV is attributed to the O 1s peak of SnO₂ patches.^{4, 5} After the PtRh@SnO₂ NW/C are annealed, a certain percentage of absorbed H₂O, O₂ and CO₂ molecules are removed, resulting in the lower intensity of the first O 1s peak.

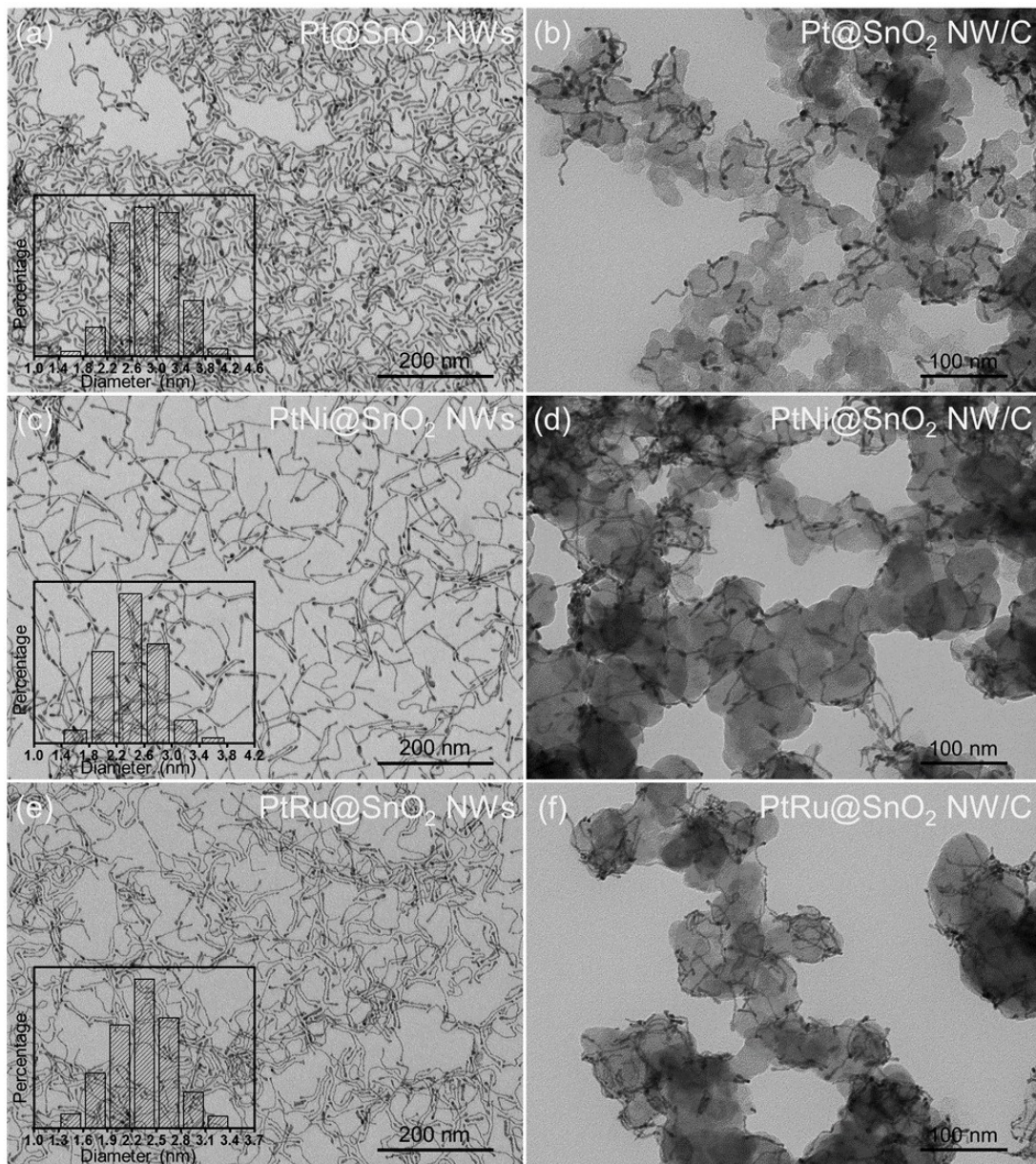


Figure S6. Additional TEM images of ultrathin Pt@SnO₂, PtNi@SnO₂ and PtRu@SnO₂ NWs (a, c, e) before and (b, d, f) after annealing treatment, respectively. The insets in (a), (c) and (e) are the diameter histograms of different NWs, which are collected by manually measuring around 200 randomly selected NWs.

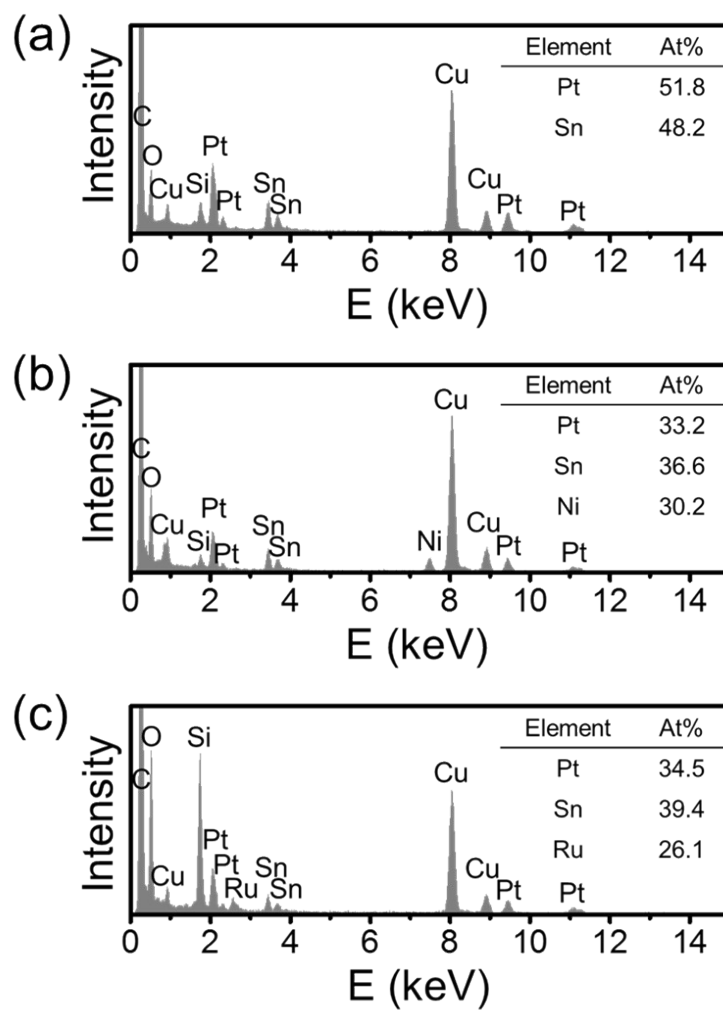


Figure S7. EDX spectra of ultrathin (a) Pt@SnO₂, (b) PtNi@SnO₂ and (c) PtRu@SnO₂ NWs.

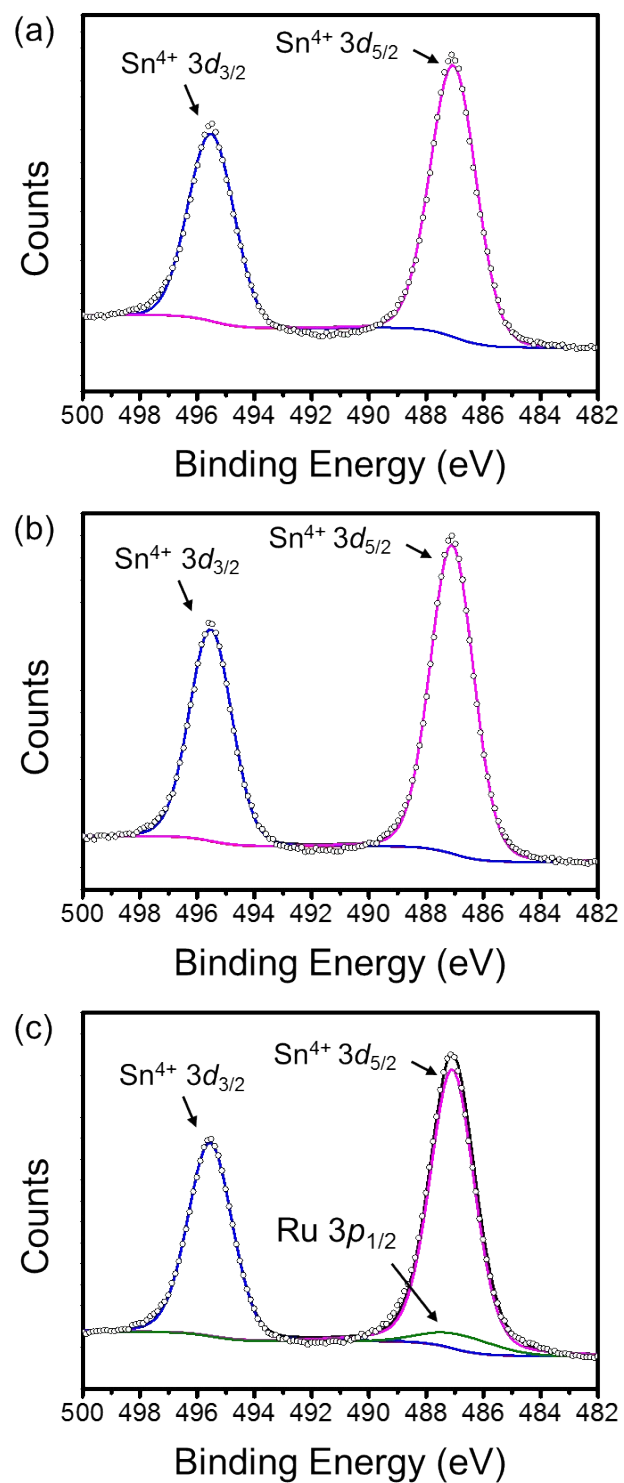


Figure S8. High-resolution Sn 3d XPS spectra of ultrathin (a) Pt@SnO₂, (b) PtNi@SnO₂ and (c) PtRu@SnO₂ NWs.

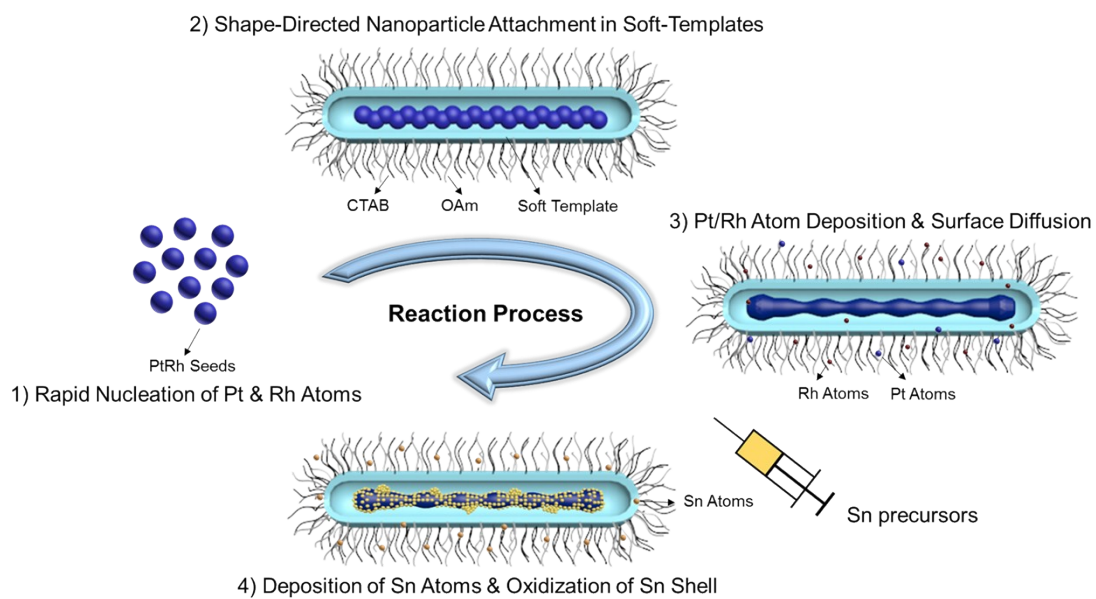


Figure S9. The schematic illustration of the growth process of ultrathin PtRh@SnO₂ NWs.

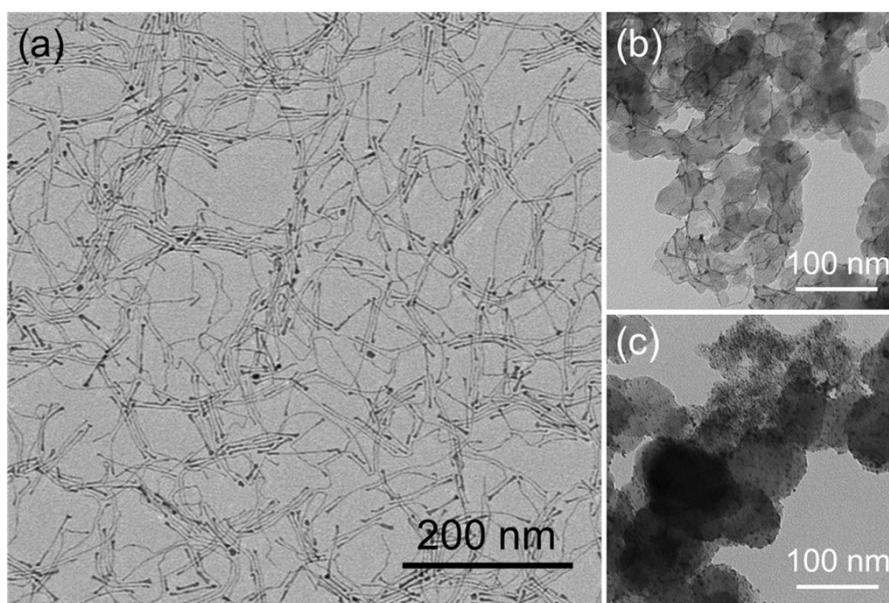


Figure S10. TEM images of (a) ultrathin Pt NWs, (b) Pt NW/C and (c) commercial Pt/C.

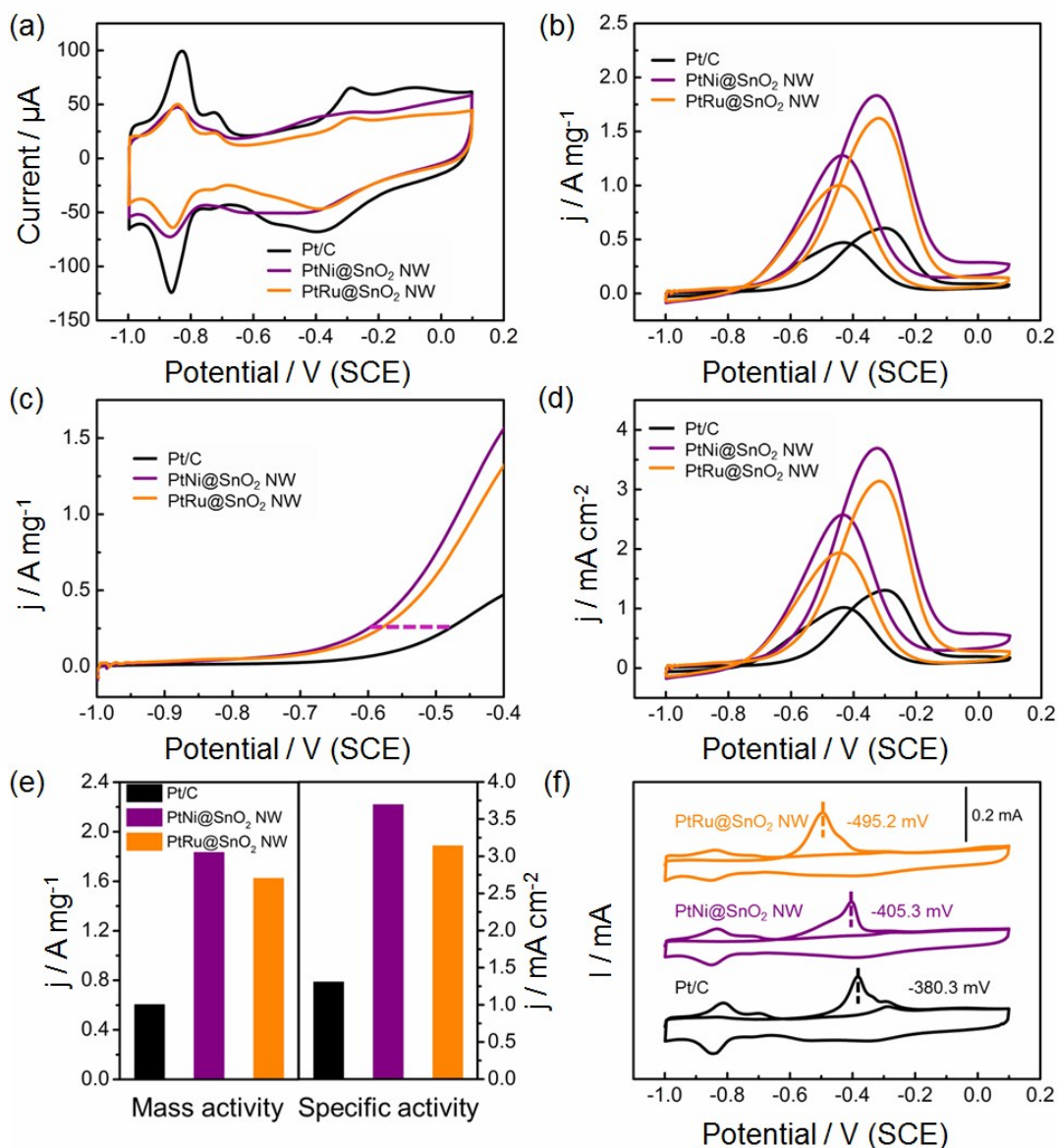


Figure S11. (a) CV curves of different catalysts in an Ar-saturated 1 M NaOH solution at a scan rate of 50 mV s^{-1} . (b) Mass-normalized CV curves of different catalysts in an Ar-saturated 1 M NaOH + 1 M ethanol solution at a scan rate of 50 mV s^{-1} . (c) Local magnified CV curves from (b). (d) ECSA-normalized CV curves of different catalysts. (e) The histograms of mass and specific activities of different catalysts. (f) CO-stripping curves of different catalysts in an Ar-saturated 1 M NaOH solution at a scan rate of 50 mV s^{-1} . Note that the peak potential of CO oxidation on PtRu@SnO₂ NW/C (-495.20 mV) is more negative than that of PtRh@SnO₂ NW/C, which is probably for the unusual catalytic behavior of Ru for CO oxidation.⁶ However, due to the low C–C bond breaking ability, the EOR activities of PtRu@SnO₂ NW/C is still lower than that of PtRh@SnO₂ NW/C.

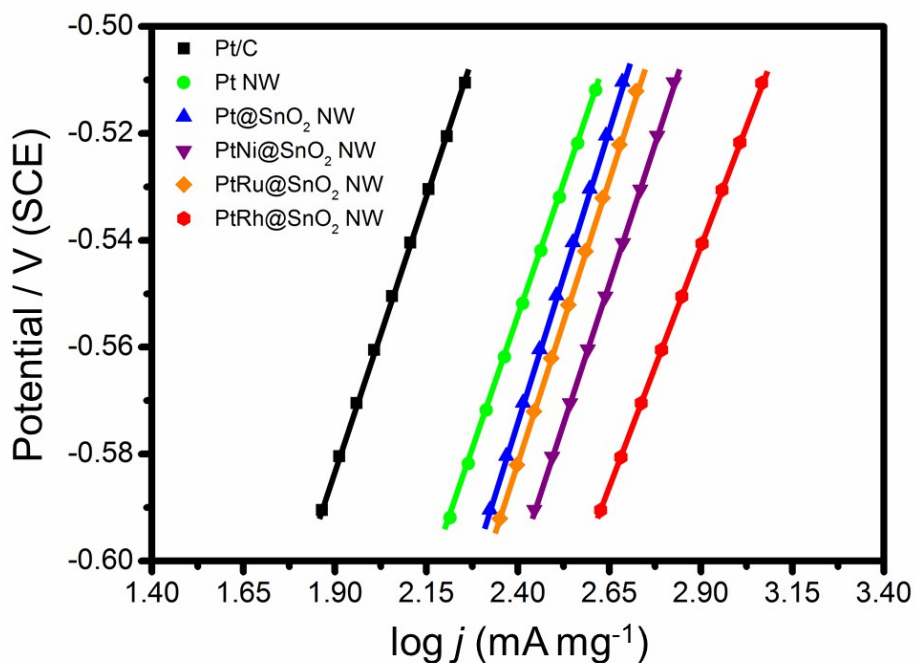


Figure S12. The Tafel plots of different catalysts including PtM@SnO₂ NWs, Pt NWs and commercial Pt/C.

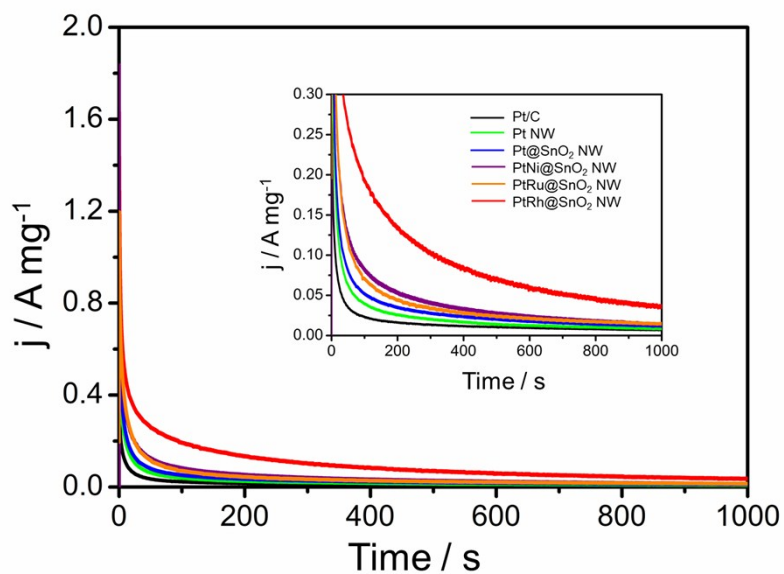


Figure S13. The chronoamperometry curves of different catalysts recorded at -0.60 V vs SCE.

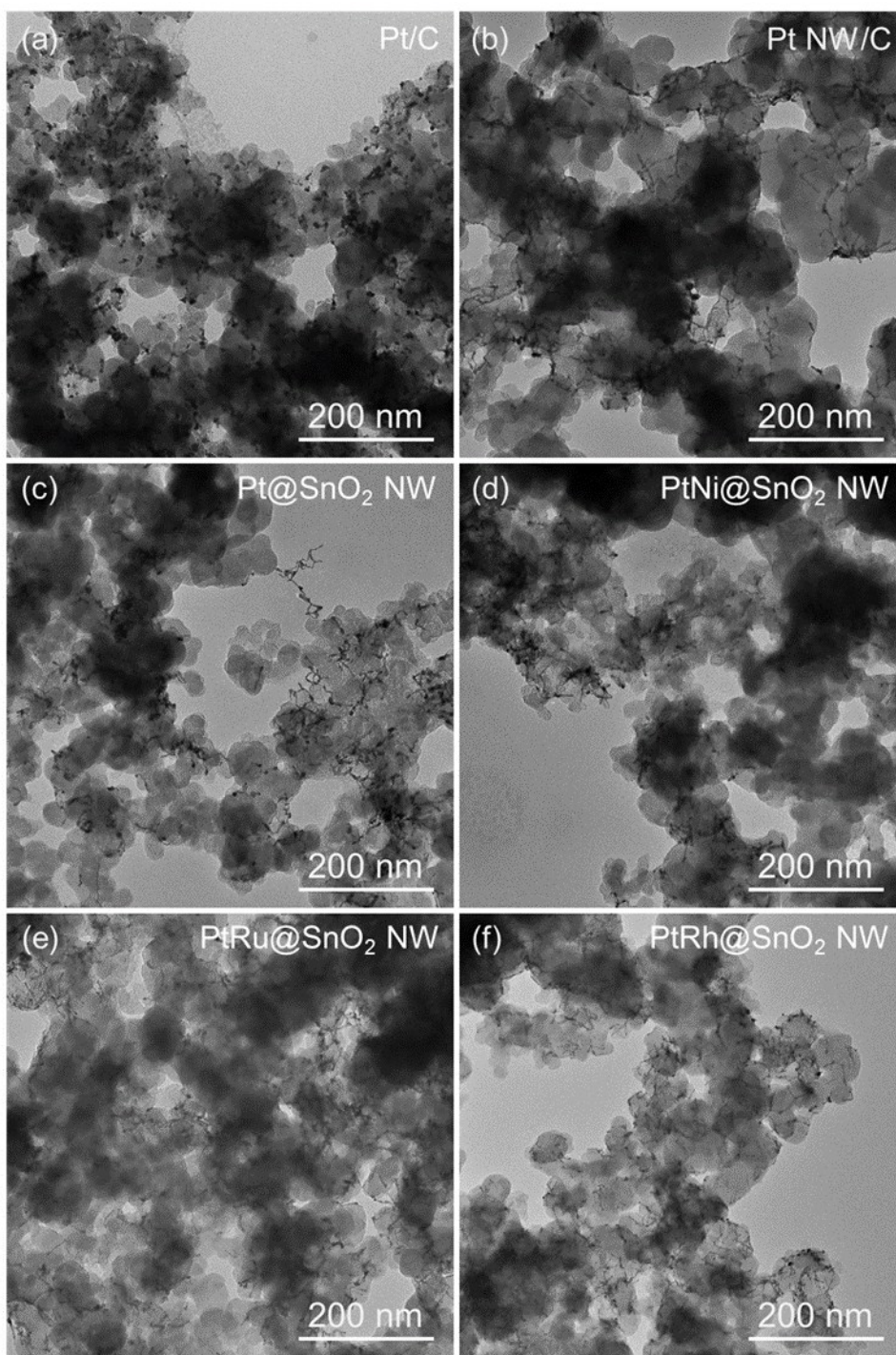


Figure S14. TEM images of different catalysts after chronoamperometry measurement.

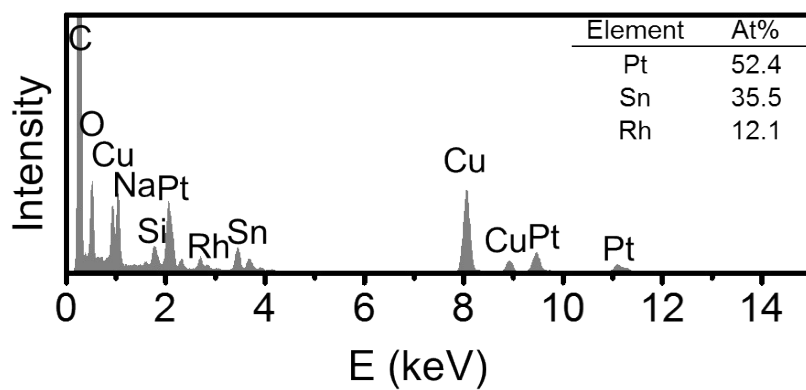


Figure S15. The EDX spectrum of PtRh@SnO₂ NW/C after chronoamperometry measurement.

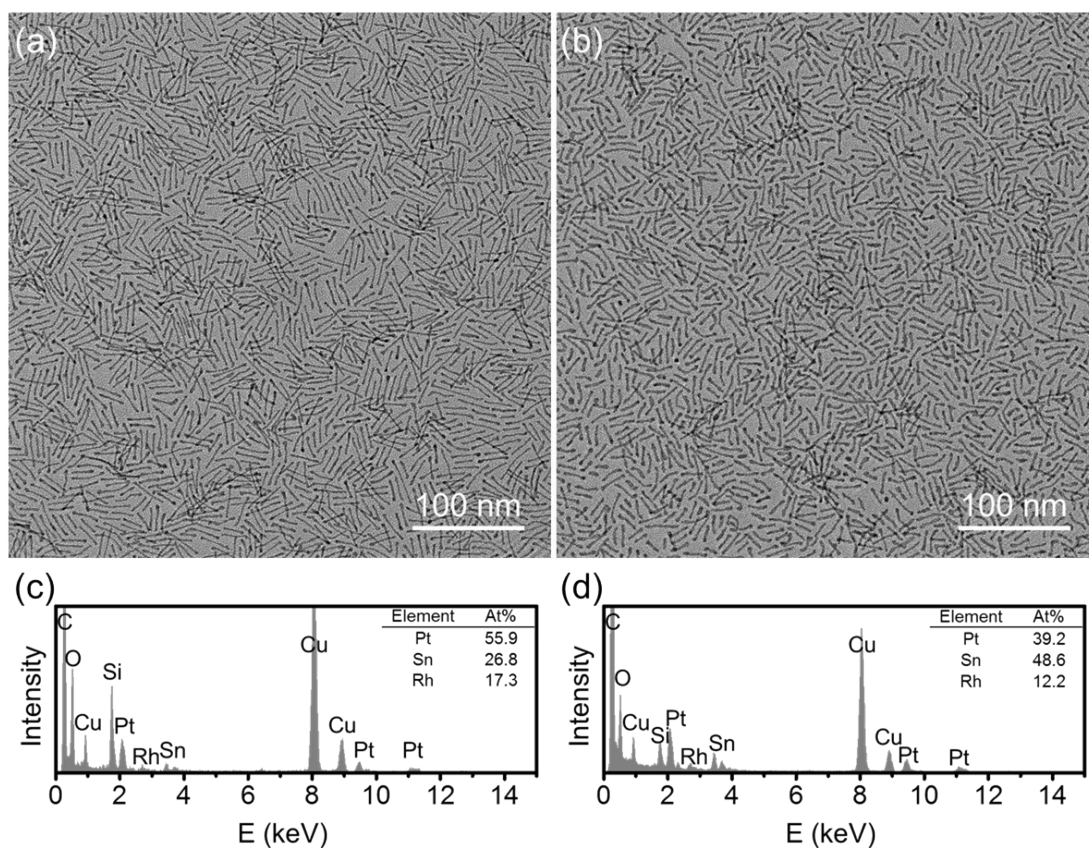


Figure S16. (a, b) Typical TEM images and (c, d) EDX spectra of PtRh@SnO₂ NWs with 26.8 at.% and 48.6 at.% Sn, respectively.

Table S1. The atomic ratios of ultrathin PtM@SnO₂ NWs characterized by EDX and ICP-MS.

Samples	EDX	ICP-MS
Pt@SnO ₂ NW (Pt:Sn)	0.52:0.48	0.47:0.53
PtNi@SnO ₂ NW (Pt:Sn:Ni)	0.33:0.37:0.30	0.28:0.39:0.33
PtRu@SnO ₂ NW (Pt:Sn:Ru)	0.35:0.39:0.26	0.33:0.41:0.26
PtRh@SnO ₂ NW (Pt:Sn:Rh)	0.46:0.41:0.13	0.46:0.39:0.15

Table S2. The EOR activities of different catalysts.

Samples	I _f /I _b	ECSA (m ² g ⁻¹)	MA (A mg ⁻¹)	SA (mA cm ⁻²)
Pt/C	1.28	46.3	0.60	1.31
Pt NW	1.13	66.2	1.37	2.07
Pt@SnO ₂ NW	1.14	47.0	1.33	2.83
PtNi@SnO ₂ NW	1.43	49.6	1.83	3.69
PtRu@SnO ₂ NW	1.62	51.7	1.62	3.14
PtRh@SnO ₂ NW	4.01	56.1	3.16	5.63

Table S3. The EOR activities of some representative Pt-based and Pd-based NWs.

Catalysts	Electrolyte	Mass Activity (A mg⁻¹)	Specific Activity (mA cm⁻²)	I_f/I_b	Ref.
PtRh@SnO ₂ NWs	1 M NaOH + 1 M ethanol	3.16	5.63	4.01	This Work
Pt ₆₉ Ni ₁₆ Rh ₁₅ NWs	0.1 M HClO ₄ + 0.5 M ethanol	1.50	2.18	1.19	7
PtRh NWs	0.1 M HClO ₄ + 0.5 M ethanol	1.55	2.08	1.17	8
PtSnRh WNWs	0.1 M NaOH + 0.1 M ethanol	0.99	NA	NA	9
Pt ₃ Co NWs	0.1 M HClO ₄ + 0.2 M ethanol	0.81	1.55	NA	10
Pt-Mo-Ni NWs	0.5 M H ₂ SO ₄ + 2 M ethanol	0.87	2.57	NA	11
PdCu NWs	1 M KOH + 1 M ethanol	3.47	NA	1.1	12
Pt ₆ Sn ₃ NWs	0.1 M HClO ₄ + 0.5 M ethanol	1.08	1.40	NA	13
PtCu _{2.1} NWs	0.1 M HClO ₄ + 0.2 M ethanol	1.02	2.16	NA	14
Pt-skin Pt ₃ Fe NWs	0.1 M HClO ₄ + 0.5 M ethanol	1.95	3.94	NA	15

NA: not available.

Reference

1. X. Fan, S. Luo, X. Zhao, X. Wu, Z. Luo, M. Tang, W. Chen, X. Song and Z. Quan, *Nano Res.*, 2019, **12**, 1721-1726.
2. V. Nefedov, D. Gati, B. Dzhurinskii, N. Sergushin and Y. Salyn, *Zh. Neorg. Khimii.*, 1975, **20**, 2307.
3. A. Pashutski, A. Hoffman and M. Folman, *Surf. Sci.*, 1989, **208**, L91-L97.
4. J. M. Wu, *J. Mater. Chem.*, 2011, **21**, 14048-14055.
5. V. Subramanian, W. W. Burke, H. Zhu and B. Wei, *J. Phys. Chem. C*, 2008, **112**, 4550-4556.
6. S. H. Joo, J. Y. Park, J. R. Renzas, D. R. Butcher, W. Huang and G. A. Somorjai, *Nano Lett.*, 2010, **10**, 2709-2713.
7. W. Zhang, Y. Yang, B. Huang, F. Lv, K. Wang, N. Li, M. Luo, Y. Chao, Y. Li, Y. Sun, Z. Xu, Y. Qin, W. Yang, J. Zhou, Y. Du, D. Su and S. Guo, *Adv. Mater.*, 2019, **31**, 1805833.
8. Y. Zhu, L. Bu, Q. Shao and X. Huang, *ACS Catal.*, 2019, **9**, 6607-6612.
9. K. Jiang, L. Bu, P. Wang, S. Guo and X. Huang, *ACS Appl. Mater. Inter.*, 2015, **7**, 15061-15067.
10. L. Bu, S. Guo, X. Zhang, X. Shen, D. Su, G. Lu, X. Zhu, J. Yao, J. Guo and X. Huang, *Nat. Commun.*, 2016, **7**, 11850.
11. J. Mao, W. Chen, D. He, J. Wan, J. Pei, J. Dong, Y. Wang, P. An, Z. Jin, W. Xing, H. Tang, Z. Zhuang, X. Liang, Y. Huang, G. Zhou, L. Wang, D. Wang and Y. Li, *Sci. Adv.*, 2017, **3**, e1601705.
12. C. Zhu, Q. Shi, S. Fu, J. Song, H. Xia, D. Du and Y. Lin, *Adv. Mater.*, 2016, **28**, 8779-8783.
13. P. Song, X. Cui, Q. Shao, Y. Feng, X. Zhu and X. Huang, *J. Mater. Chem. A*, 2017, **5**, 24626-24630.
14. N. Zhang, L. Bu, S. Guo, J. Guo and X. Huang, *Nano Lett.*, 2016, **16**, 5037-5043.
15. M. Luo, Y. Sun, X. Zhang, Y. Qin, M. Li, Y. Li, C. Li, Y. Yang, L. Wang, P. Gao, G. Lu and S. Guo, *Adv. Mater.*, 2018, **30**, 1705515.